

The alternative oxidase lowers mitochondrial reactive oxygen production in plant cells

DENIS P. MAXWELL*, YONG WANG*, AND LEE MCINTOSH*†‡

*Department of Energy Plant Research Laboratory, and †Department of Biochemistry, Michigan State University, East Lansing, MI 48824

Communicated by Hans J. Kende, Michigan State University, East Lansing, MI, May 17, 1999 (received for review February 12, 1999)

ABSTRACT Besides the cytochrome *c* pathway, plant mitochondria have an alternative respiratory pathway that is comprised of a single homodimeric protein, alternative oxidase (AOX). Transgenic cultured tobacco cells with altered levels of AOX were used to test the hypothesis that the alternative pathway in plant mitochondria functions as a mechanism to decrease the formation of reactive oxygen species (ROS) produced during respiratory electron transport. Using the ROS-sensitive probe 2',7'-dichlorofluorescein diacetate, we found that antisense suppression of AOX resulted in cells with a significantly higher level of ROS compared with wild-type cells, whereas the overexpression of AOX resulted in cells with lower ROS abundance. Laser-scanning confocal microscopy showed that the difference in ROS abundance among wild-type and AOX transgenic cells was caused by changes in mitochondrial-specific ROS formation. Mitochondrial ROS production was exacerbated by the use of antimycin A, which inhibited normal cytochrome electron transport. In addition, cells overexpressing AOX were found to have consistently lower expression of genes encoding ROS-scavenging enzymes, including the superoxide dismutase genes *SodA* and *SodB*, as well as glutathione peroxidase. Also, the abundance of mRNAs encoding salicylic acid-binding catalase and a pathogenesis-related protein were significantly higher in cells deficient in AOX. These results are evidence that AOX plays a role in lowering mitochondrial ROS formation in plant cells.

All organisms produce a range of reactive oxygen species (ROS), including superoxide ($\cdot\text{O}_2^-$), the hydroxyl radical ($\cdot\text{OH}$), and hydrogen peroxide (H_2O_2), during the course of normal metabolic processes. If not effectively and rapidly removed from cells, ROS can damage a wide range of macromolecules, possibly leading to cell death. Both enzymatic and nonenzymatic mechanisms have evolved to protect cells from oxygen toxicity. These include antioxidants such as ascorbate and glutathione, as well as ROS-scavenging enzymes such as superoxide dismutase (SOD), catalase, and peroxidase (1).

Mitochondria are a major source of ROS in eukaryotic cells. In humans, aberrant mitochondrial ROS formation has been associated with conditions such as Parkinson's disease, amyotrophic lateral sclerosis, and aging (2). Superoxide, which is rapidly converted to H_2O_2 through the action of SOD, is produced during respiration primarily by the autooxidation of reduced mitochondrial electron-transport components (3). One of these components, a major site of superoxide production along the respiratory chain, is the ubiquinone pool (3). The formation of superoxide is exacerbated by compounds, such as antimycin A, that block electron transport downstream of the ubiquinone pool (3).

Unlike animal mitochondria, those of plants possess a bifurcated electron-transport chain. In addition to the cytochrome respiratory pathway found in all eukaryotes, plants have a second, alternative pathway that diverges from the main respiratory chain at ubiquinone (4). Electron flow through the alternative pathway bypasses two of the three sites along the cytochrome chain where electron transport is coupled to ATP synthesis. The alternative pathway is comprised of a single protein, alternative oxidase (AOX; ref. 5), which is thought to exist in the inner mitochondrial membrane as a homodimer (6). In all species examined, AOX is encoded by a small family of nuclear genes whose members are differentially regulated in a developmental and tissue-specific manner (see ref. 4 and references therein). Disruption of the cytochrome pathway leads to induction of AOX in many organisms. For example, the addition of antimycin A to cultured tobacco cells resulted in the induction of both AOX mRNA (7) and protein (8). The overexpression in tobacco of *Aox1*, a nuclear gene encoding AOX, led to a large increase in AOX protein and alternative pathway capacity, whereas antisense inhibition of *Aox1* effectively reduced AOX protein to undetectable levels (9). Further work with these transgenic plants showed that changes in the level of AOX within the mitochondria did not have a significant effect on growth rate, except in the presence of antimycin A (10). Under those conditions, cells overexpressing *Aox1* grew significantly faster than wild type (WT), whereas cells with suppressed levels of AOX died.

Although AOX is found in all plants investigated to date, as well as in some fungi and protists, its only confirmed function occurs in the thermogenic inflorescence of the Araceae (4). Recently, however, it has been proposed (11, 12) that AOX may serve a more general function in all plant species by limiting mitochondrial ROS formation. An experimental basis for this hypothesis is that conditions that induce AOX expression, including chilling (13), pathogen attack (14), aging (15), and inhibition of the cytochrome pathway (8), also cause an increase in cellular ROS formation (16–18). Because stress-induced physical changes in membrane components may lead to a restriction in cytochrome pathway respiration (19) and thus increase ROS formation, the presence of a second quinol oxidase may help to prevent overreduction of upstream electron-transport components. In so doing, alternative pathway respiration would also continue to reduce oxygen to water and thus keep the intracellular concentration of this potential toxin low.

This study sought to test the hypothesis that AOX may serve to keep mitochondrial ROS formation low. Our goal was to measure ROS formation in intact cells rather than isolated

The publication costs of this article were defrayed in part by page charge payment. This article must therefore be hereby marked "advertisement" in accordance with 18 U.S.C. §1734 solely to indicate this fact.

PNAS is available online at www.pnas.org.

Abbreviations: DCF, dichlorofluorescein; H_2DCF , 2',7'-DCF; $\text{H}_2\text{DCF-DA}$, 2',7'-dichlorofluorescein diacetate; ROS, reactive oxygen species; SOD, superoxide dismutase; WT, wild type; GPX, glutathione peroxidase; SA-Cat, salicylic acid-binding catalase; RT-PCR, reverse transcription-PCR; BHA, butylated hydroxyanisole; S11, containing *Aox1* in sense orientation; AS8, containing *Aox1* in antisense orientation.

‡To whom reprint requests should be addressed. e-mail: mcintos1@pilot.msu.edu.

mitochondria to gain a more biologically accurate assessment of mitochondrial ROS formation as it occurs *in vivo*. To meet our goals, we used heterotrophically grown tobacco cells that overexpress or underexpress *Aox1*. Although these cells lack developed chloroplasts, which themselves represent a major source of ROS within plants, our system has the experimental advantage of enabling one to estimate mitochondrial ROS formation more easily and arguably more accurately within plant cells through the use of fluorescent probes and confocal microscopy.

MATERIALS AND METHODS

Plant Material and Growth Conditions. Cultured tobacco cells (*Nicotiana tabacum* cv. Petit Havana SR1) containing *Aox1* in either sense (S11) or antisense (AS8) orientation have been characterized (9, 10). All experiments were conducted with exponentially growing cells 3–4 days after subculture.

Detection of Reactive Oxygen Species. Spectrofluorometry. Intracellular production of ROS was measured by using 2',7'-dichlorofluorescein diacetate (H₂DCF-DA; Molecular Probes). This nonpolar compound is converted to the membrane-impermeant polar derivative H₂DCF by esterases when it is taken up by the cell. H₂DCF is nonfluorescent but is rapidly oxidized to the highly fluorescent DCF by intracellular H₂O₂ and other peroxides (20). Stocks of H₂DCF-DA (5 mM) were made in ethanol and stored in the dark at –80°C under argon. H₂DCF-DA was added to cells at a final concentration of 5 μ M. After a 30-min incubation, cells were collected in a microcentrifuge, and the supernatant was removed and diluted 50-fold. Fluorescence was measured by using a Hitachi F2000 fluorescence spectrophotometer (Tokyo) with excitation and emission wavelengths set at 488 nm and 520 nm, respectively.

Laser-scanning confocal microscopy. An InSight Bilateral Laser-Scanning confocal microscope (Meridian Instruments, Okemos, MI; ref. 21) was used with an air-cooled, argon-ion laser as the excitation source. Cells were washed once in growth medium and then loaded with H₂DCF-DA (15 μ M) and Mitotracker Red (0.5 μ M; Molecular Probes), a dye that is specifically taken up by metabolically active mitochondria (22). Antimycin A (5 μ M) was added 5 min before the dyes. DCF was excited at 488 nm and detected through a 530/30-nm bandpass filter. Mitotracker Red was excited at 568 nm and detected through a >665-nm long-pass filter. Laser intensity was identical for all experiments and set at minimum (8–10%) because of the very high fluorescent signal from AS8 cells incubated with antimycin A. Data were collected by a dedicated instrument computer and stored on the hard drive. Data were imported into ADOBE PHOTOSHOP 4.0 for preparation of figures.

RNA Isolation and Gel Blot Analyses. Total cellular RNA was isolated and separated on formaldehyde-containing agarose gels and analyzed by blotting as described (7). Hybridization probes were as follows: *N. tabacum* glutathione peroxidase (GPX; ref. 23); *Nicotiana plumbaginifolia* *SodA*, encoding the mitochondrial SOD isozyme MnSOD; *SodB*, encoding the chloroplastic SOD isozyme FeSOD; and *SodCc*, encoding the cytosolic Cu/Zn-SOD (24). A salicylic acid-binding catalase (SA-Cat) partial cDNA (834-bp) of *N. tabacum* was obtained by reverse transcription-PCR (RT-PCR) as described (25). A 475-bp fragment of *N. tabacum* pathogenesis-related gene 1 (PR-1) cDNA was also obtained by using RT-PCR. The PR-1 specific primers 5'-ATTGCCTTCATTCTTCTTGCT-3' and 5'-GACTTTCTCCTCTATAATACCTG-3' were selected based on a published cDNA sequence (26). Identity of both SA-Cat and PR-1 were confirmed at the Michigan State University DNA sequencing facility by using an Applied Biosystems Prism 377 DNA sequencer. A 300-bp fragment of the *Arabidopsis* translation initiation factor

elF4A (27) was used to confirm the equal loading of RNA. Blots were quantified by densitometry.

Total Protein Determination. Total cellular protein was isolated as described (28), and protein concentrations were determined by using a BCA protein assay kit (Pierce).

Chemicals. Antimycin A, butylated hydroxyanisole (BHA), flavone, and menadione were obtained from Sigma. Each was dissolved in an appropriate solvent at a concentration 1,000-fold greater than the final concentration. Mitotracker Red and H₂DCF-DA were obtained from Molecular Probes.

RESULTS

Detection of Intracellular ROS in Intact Tobacco Cells. The chemical probe H₂DCF-DA has been used extensively as a noninvasive, *in vivo* measure of intracellular ROS (20). H₂DCF-DA was used here to determine whether changes in the intracellular level of ROS correlated with the abundance of AOX in mitochondria. As shown in Fig. 1, the level of DCF fluorescence was approximately five times greater in cells with suppressed AOX levels (AS8) compared with WT cells, whereas the level of DCF fluorescence in cells overexpressing AOX (S11) was 57% lower than that of WT cells.

Inhibition of Mitochondrial Electron Transport Increases ROS Production *in Vivo*. It has been shown in isolated animal mitochondria that chemical inhibition of electron transport results in increased superoxide formation (3). However, with isolated plant mitochondria, superoxide production was found to depend highly on the substrate(s) used to drive electron transport during the assay (11, 29). Because of this variability, the actual extent of mitochondrial superoxide production in intact plant cells remains unclear. Antimycin A is often used in animal (30) and plant (8) cells to study the effects of respiratory inhibition on cellular processes. Addition of antimycin A to tobacco cell cultures resulted in an increase in intracellular ROS as measured by DCF fluorescence in all cell lines (Fig. 2). Both the rate of production and abundance of ROS produced as a consequence of inhibiting cytochrome electron transport were inversely related to the presence of AOX. S11 cells had \approx 3.7-fold lower DCF fluorescence, whereas AS8 cells had 2.5 times greater fluorescence compared with WT cells after the 4-h antimycin A treatment.

Intracellular Localization of ROS Production. The differences in ROS production among the cell lines as determined

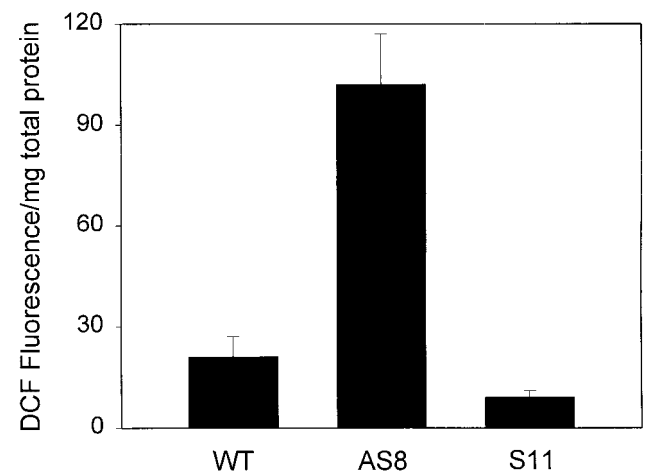


Fig. 1. Intracellular ROS abundance in WT and *Aox1* transgenic cultured tobacco cells. Intracellular ROS was measured by using H₂DCF-DA as described in *Materials and Methods*. Measurements were made by using cells 3–4 days after subculture. Results represent the means (\pm SD) of six to eight separate experiments. AS8, *Aox1* antisense; S11, *Aox1* overexpressor.

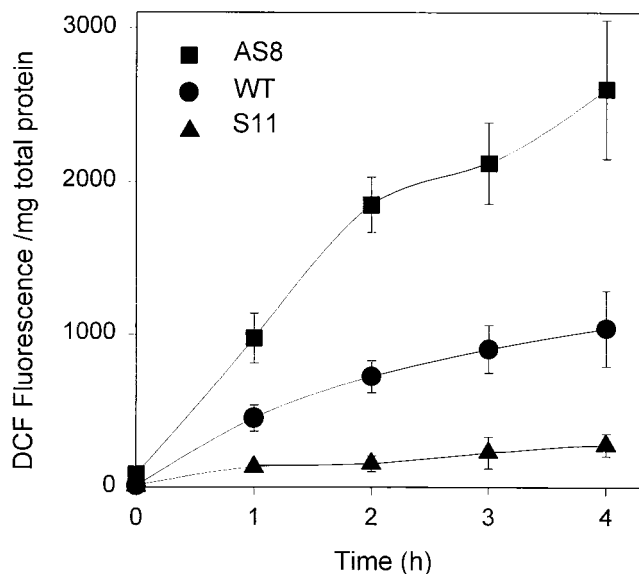


Fig. 2. ROS formation in WT and *Aox1* transgenic cultured tobacco cells after inhibition of cytochrome *c* electron transport. Time course of ROS production after addition of antimycin A ($5 \mu\text{M}$) to intact cells at $t = 0$. At each time point, an aliquot of cells was removed and incubated with $\text{H}_2\text{DCF-DA}$ for 30 min before fluorescence measurement. ●, WT; ■, AS8; ▲, S11. Results represent the means (\pm SD) of four separate experiments.

by spectrofluorometry were confirmed by using laser-scanning confocal microscopy (Fig. 3). Under normal growth conditions, only AS8 gave a detectable DCF signal, indicative of a basal ROS level that exceeds that of WT or S11 cells. Low-level DCF fluorescence was detected in control WT and S11 cells when the fluorescence signals were amplified to such an extent that AS8 images were rendered overexposed (data not shown). The addition of antimycin A to AS8 and WT cells resulted in a large increase in DCF fluorescence from punctate sources within the cell. Even on addition of antimycin A, we could not detect a significant increase in DCF fluorescence with S11 cells by using the chosen low laser intensity. To confirm that the major sites of ROS formation within the tobacco cells were mitochondria, cells were double-stained with $\text{H}_2\text{DCF-DA}$ and the mitochondria-specific dye Mitotracker Red. Mitotracker dyes have been used with cultured tobacco cells to confirm the mitochondrial localization of green fluorescent protein-tagged constructs (22). Cells from each line were found to have comparable Mitotracker staining regardless of antimycin A pretreatment or the presence of a DCF signal (Fig. 3). When detectable, the intracellular localization of the DCF signal exactly matched that of the Mitotracker signal, resulting in a single yellow image when the red Mitotracker signal was merged with the green DCF signal (data not shown).

Extramitochondrial Sources of ROS and ROS Scavenging. Because antimycin A is specific for increasing mitochondrial ROS formation, we wanted to extend our investigation by examining the response of each cell line to ROS produced outside the mitochondria. Both H_2O_2 and menadione, a redox cycling quinone that generates superoxide *in vivo*, are commonly used to raise the ROS level within plant cells (31). Addition of either of these compounds caused a significant increase in intracellular ROS in all three cell lines (Fig. 4A). As was observed with antimycin A, the addition of H_2O_2 or menadione caused the greatest increase in DCF fluorescence in AS8 cells. However, unlike antimycin A, the addition of H_2O_2 to S11 cells caused a rise in intracellular ROS comparable to WT cells, whereas the addition of menadione to S11 cells resulted in an ROS level that was three times greater than that seen in WT cells.

It has been shown in many systems that treating cells with antioxidants lowers ROS abundance. In the yeast *Hansenula anomala*, the antimycin A-induced increase in AOX abundance was inhibited by pretreating cells with the antioxidants BHA or flavone (32). In our experiments, intracellular ROS production by addition of antimycin A was lowered $\approx 52\%$ in AS8 to $\approx 90\%$ in S11 when the cells were pretreated with BHA ($100 \mu\text{M}$) or flavone (0.5 mM ; Fig. 4B). Addition of the membrane-impermeable ROS-scavenging enzymes catalase and SOD had no effect on DCF fluorescence levels (data not shown).

ROS-Scavenging Enzyme Profiles. A variety of stress conditions are known to increase the expression of genes encoding ROS-scavenging enzymes. We investigated whether altered AOX levels, and consequently altered mitochondrial ROS production, changed the expression of major ROS-scavenging enzymes (Fig. 5A). Transgenic plants overexpressing certain SOD isozymes show increased tolerance to oxidative conditions, including ozone (33) and freezing stress (34). Transcript abundance of the *SodA* gene, which encodes the mitochondrial isozyme MnSOD, was found to be comparably high in both WT and AS8 cells, whereas S11 consistently showed approximately 3-fold lower expression (Fig. 5A). The high level of MnSOD expression seen in cell culture has been observed previously (35) and was found to be directly related to high levels of sucrose in the medium, giving rise to high respiration rates. Although the cells used in these experiments were grown heterotrophically and thus lacked developed chloroplasts, we found significant expression of *sodB*, the gene encoding a chloroplastic SOD isozyme, FeSOD (Fig. 5B). That high *sodB* expression can occur in the absence of fully functional chloroplasts has been shown previously (36). The expression of *SodCc*, encoding cytosolic Cu/Zn SOD, remained essentially unchanged by alterations in the abundance of AOX (data not shown).

The H_2O_2 produced through the action of SOD is converted to O_2 and H_2O through the action of catalase. It has been shown that reduction in catalase levels in tobacco leads to increased necrosis and the activation of disease resistance (37). As shown in Fig. 5A, cells deficient in AOX (AS8) showed very high mRNA levels of SA-Cat (38), whereas expression of this gene was barely detectable in WT or S11 cells. Previously, we observed an expression profile almost identical to SA-Cat when the *N. plumbaginifolia* Cat2 (39) cDNA was used as a probe (40).

Expression of the *N. tabacum* gene encoding the cytosolic form of GPX (23) has been shown to increase in plants exposed to environmental stresses. In this study, the level of GPX transcripts was approximately 3-fold greater in AS8 compared with WT, whereas it was almost undetectable in S11 cells.

PR genes show induced expression after pathogen attack. This induction can be mimicked in tobacco leaves by injection of H_2O_2 or of compounds that increase H_2O_2 levels, such as salicylic acid or the catalase inhibitor 3-amino triazole (38). In support of our experimental evidence that altering *Aox1* expression leads to changes in intracellular ROS abundance, we found that the transcript abundance of the PR-1 gene was approximately four to five times greater in AS8 compared with WT, whereas expression was undetectable in S11 cells (Fig. 5B).

DISCUSSION

It has been proposed that alternative pathway respiration may serve to lower ROS production in plant mitochondria (11, 12). The establishment of transgenic tobacco suspension cells that have constitutively high expression of AOX and others with suppressed levels has enabled us to test this hypothesis directly. Taken together with previous work in which the abundance of AOX in WT and transgenic cells was determined (9), the data

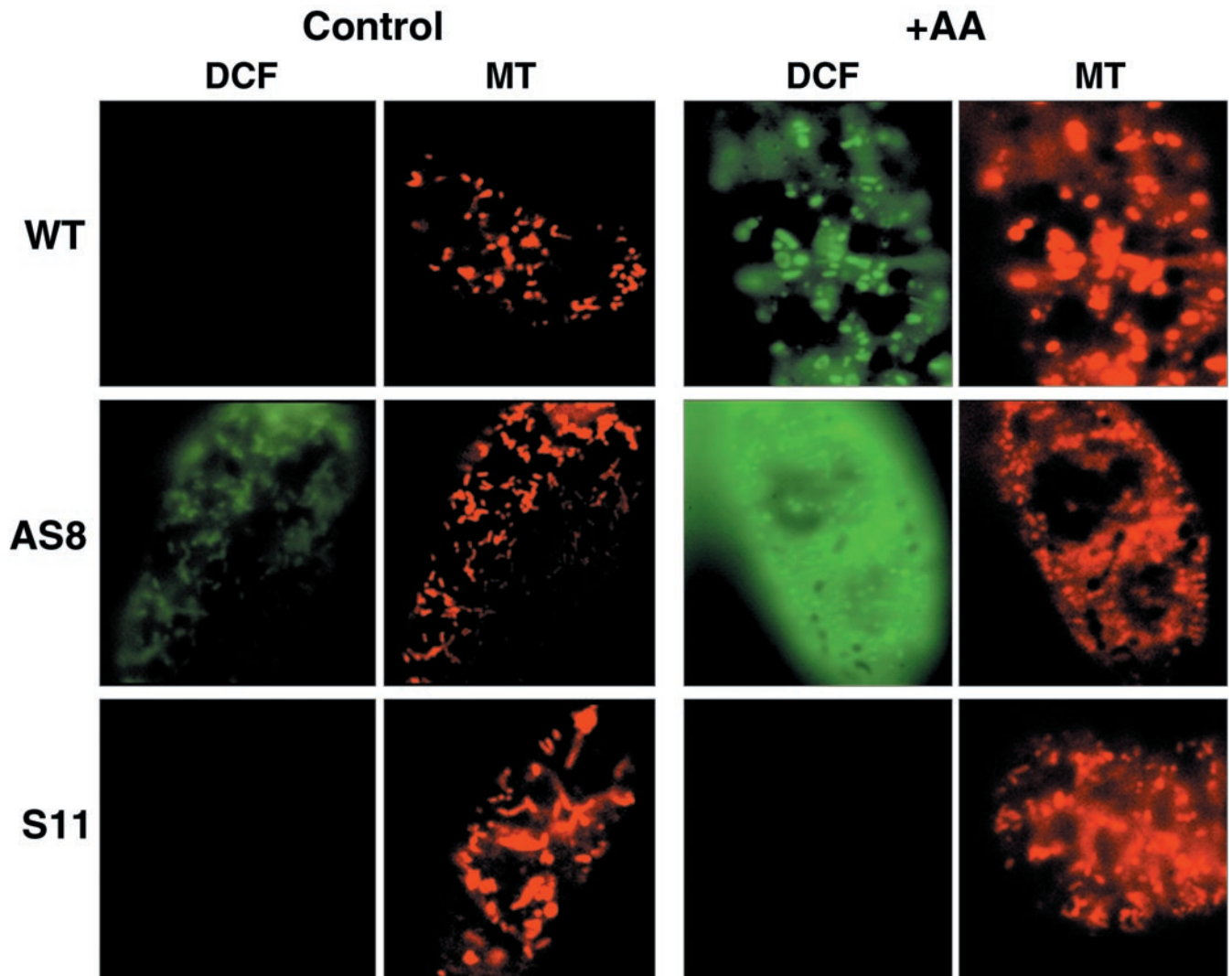


FIG. 3. Intracellular localization of ROS formation. Laser-scanning confocal microscope images of WT and *Aox1* transgenic cultured tobacco cells. Cells were double-labeled with H₂DCF-DA and Mitotracker Red. If used, antimycin A (+AA) was added 5 min before the dyes. Magnification for all images was $\times 350$.

presented here show the existence of an inverse relationship between the abundance of AOX within the mitochondria and the level of ROS found in the plant cell. The biological importance of this finding lies in the fact that ROS are potentially very toxic, being produced in excess when plants are subjected to stress conditions such as chilling and pathogen attack. A more complete understanding of the mechanisms that lower ROS formation should aid in the development of plants with higher resistance to both biotic and abiotic stresses.

Our results with transgenic cells are in accordance with a recent study (41) in which it was shown that inhibition of alternative pathway respiration by addition of salicylhydroxamic acid to isolated soybean mitochondria caused an increase in H₂O₂ production, as measured by oxidation of H₂DCF-DA. However, salicylhydroxamic acid has been shown to react directly with H₂DCF-DA (42) and is known to inhibit certain enzymes including peroxidases (17). Because of these concerns, we avoided its use in our experiments, relying instead on intact cells with genetically altered levels of AOX.

The method applied here to detect intracellular oxidative stress is based on the oxidation of H₂DCF-DA to fluorescent DCF by H₂O₂ and organic peroxides (30). H₂DCF-DA is not oxidized by superoxide (20). H₂DCF-DA has been used as a "specific" probe for intracellular H₂O₂ in a wide variety of organisms, including animal cells, to study the antimycin

A-induced increase in mitochondrial H₂O₂ production (30, 43). In plants, H₂DCF-DA has been employed to monitor H₂O₂ release after pathogen attack in soybean suspension cells (44) and as an indicator of oxygen-radical production in soybean roots after iron supplementation (45).

The use of the mitochondrial-specific marker Mitotracker Red in combination with laser-scanning confocal microscopy allowed us to identify the mitochondria as the major site of DCF fluorescence and, thus, ROS formation in these cells. Increased fluorescence is most clearly seen in WT cells (Fig. 3), in which addition of antimycin A caused a dramatic increase in the DCF signal that originates from punctate sources within the cell. These sources were identified as mitochondria, because the mitochondrial-specific marker Mitotracker Red had an identical intracellular localization. The diffuse confocal image seen after the addition of antimycin A to AS8 cells (Fig. 3) is very likely the result of excessive H₂O₂ formation in combination with its rapid diffusion out of the mitochondria before reacting with H₂DCF. These experiments show that a restriction in mitochondrial electron transport leads to increased ROS formation *in vivo* in plants.

Our finding that mitochondria are a major source of ROS in plant cells supports a model (46) in which H₂O₂ is proposed to act as a secondary messenger in a signal transduction pathway from mitochondria to the nucleus. Support for this hypothesis

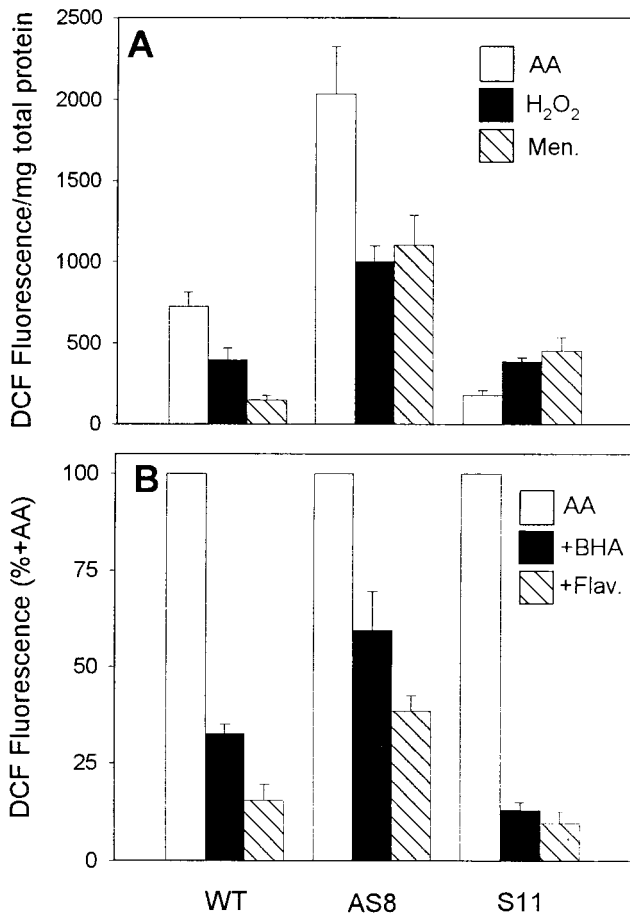


FIG. 4. Effects of ROS-generating and ROS-scavenging compounds on intracellular ROS levels. (A) Cells were incubated for 4 h in the presence of the ROS-generating compounds antimycin A (AA; 5 μ M), H₂O₂ (1 mM), or menadione (Men.; 100 μ M) before ROS determination. (B) Effect of common antioxidants on the antimycin A-dependent increase in DCF fluorescence. Cells were preincubated for 1 h with either BHA (100 μ M) or flavone (+Flav.; 0.5 mM) before the addition of antimycin A (AA). DCF fluorescence was determined 4 h after the addition of antimycin A. Data are presented as percentages of the absolute values shown in A. Results represent the means (\pm SD) of three separate experiments.

includes the finding that the expression of *Aox1*, a nuclear gene, is enhanced within minutes after the cytochrome pathway is inhibited by antimycin A treatment (7). The induction of *Aox1* by antimycin A may prove to be a model in investigating the underlying mechanism(s) of the retrograde signaling pathway between mitochondria and the nucleus in plants. The data presented here clearly suggest a role for H₂O₂ as a retrograde signaling molecule.

The changes in mitochondrial ROS production among the three cell lines correlate with changes seen in the expression profile of genes encoding ROS-scavenging enzymes. In cells overexpressing *Aox1* (S11), decreased expression levels, compared with WT, were found for a number of genes, including the mitochondrial SOD gene *SodA* but also *SodB* and GPX (Fig. 5A), which encode extramitochondrial proteins. This decrease in the expression of ROS-scavenging genes in S11 cells suggests that, although they have a higher level of AOX and consequently are more resistant to antimycin A-induced ROS formation, S11 cells may be more susceptible than WT to ROS produced independently of mitochondrial electron transport. Support for this idea comes from the finding that, on the addition of menadione, S11 cells show an increase in ROS formation that is 3 times that of WT (Fig. 4A). These findings illustrate that changing mitochondrial ROS formation may

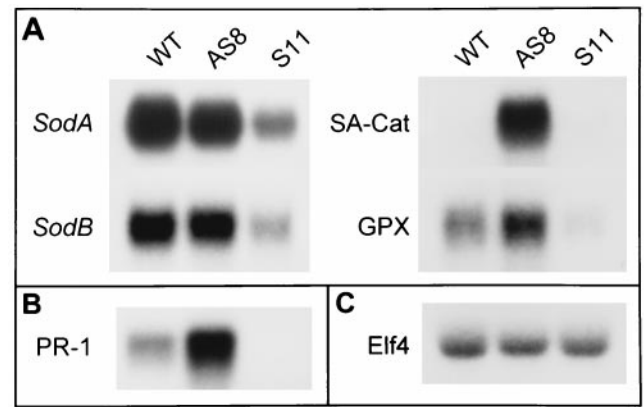


FIG. 5. Expression of genes encoding ROS-scavenging enzymes and PR-1 in WT and *Aox1* transgenic cells. RNA gel blot analysis of 25 μ g of total RNA isolated from cultured tobacco cells 3–4 days after subculture. (A) Probes for ROS-scavenging transcripts were *SodA* and *SodB* from *N. plumbaginifolia*, GPX from *N. tabacum*, and SA-Cat from *N. tabacum*; probes were obtained by RT-PCR. (B) PR-1 from *N. tabacum* was obtained by RT-PCR. (C) *Arabidopsis* translation initiation factor *elf4A* was used to confirm equal loading of RNA.

affect ROS scavenging as well as other processes throughout the cell. Whereas antisense suppression of AOX resulted in cells (AS8) with higher ROS abundance than WT, the expression level of most of the ROS-scavenging genes is about the same. This result suggests that a further increase in the expression of ROS-scavenging genes may not be possible and that regulation may occur at the level of translation or enzyme activity. An exception to this finding is the specific induction of the catalase gene SA-Cat in AS8 cells alone. Although AS8 cells show strong induction of this gene, they show the greatest increase in DCF fluorescence when subjected to H₂O₂ or menadione treatment (Fig. 4A). A likely explanation for this result, supported by our data, is the fact that the lack of AOX in AS8 and consequential increase in mitochondrial ROS formation taxes the antioxidant system to an extent that the cells cannot effectively cope with additional ROS generation.

Regardless of cell line, the ROS produced by addition of antimycin A could be at least partially countered by addition of chemical antioxidants (Fig. 4B). Although the increase in ROS was almost completely inhibited in S11 cells by antioxidant treatment, inhibition was not as effective in AS8 or WT. This result was probably due to the far greater overall ROS formation in WT and AS8 cells.

The specific role of SA-Cat in plant cells is unknown. Based on phylogenetic analysis of DNA sequences, SA-Cat of *N. tabacum* and Cat2 from *N. plumbaginifolia* form a discrete group well separated from other dicot catalases (39). This phylogenetic separation may indicate that Cat2 and SA-Cat serve a specific function quite distinct from other catalases in the cell. Both SA-Cat and PR-1 have been shown to be induced by stresses that generate ROS (25, 40), and both proteins are involved in the establishment of plant defenses against pathogen attack (40). Although the induction of SA-Cat and PR-1 in cells with suppressed AOX expression may simply be a response to greater ROS formation, their induction may reflect an underlying role for AOX in pathogen defense. Indeed, not only is AOX induced by pathogens (14) but it has recently been proposed that alternative pathway respiration is required for the establishment of resistance to tobacco mosaic virus (47). Induction of AOX is likely mediated by the oxidative burst of H₂O₂ at the cell wall during initial pathogen invasion. The oxidative burst has been shown to act as a signal resulting in the activation of a defense response in neighboring cells (43). As part of this defense response, increased expression of AOX and concomitant increase in alternative pathway

respiration may serve to maintain mitochondrial function and, thus, play a role in preventing the death of cells surrounding the initial site of infection.

Although the work described in this paper used heterotrophically grown plant cells without developed chloroplasts, it is the chloroplast that is most often viewed as the major source of ROS within the plant. However, recent work with maize (48) has challenged this notion by showing that an increase in leaf H₂O₂ content found on chilling was independent of the irradiance used during the experiment. Because the plant cell contains chloroplast-specific isozymes for many antioxidant enzymes, the extent to which ROS produced within the chloroplast affects other cellular compartments may be minimal. This recent finding on the effect of chilling on maize implicates other sites in the plant cell, including the mitochondria, as major sources of H₂O₂ formation during stress.

The findings described in this paper show that AOX plays a role in lowering ROS formation in plant mitochondria. Besides mediating the transient temperature rise in Araceae, this function of AOX in plants is the only one that has experimental support. The most plausible explanation for why AOX may lower ROS levels is that a second oxidase downstream of the ubiquinone pool maintains upstream electron-transport components in a more oxidized state, thereby lowering ROS generation by overreduced electron carriers. The higher level of ROS and the increased expression of ROS-sensitive genes, such as PR-1 and SA-Cat, in cells with suppressed AOX levels (AS8) support this claim. Based on this work, we propose that AOX should be considered alongside other enzymes, such as SOD and catalase, as a mechanism by which plants can protect themselves from oxidative stress.

We thank Melvin Schindler for the use of his confocal microscope, Sharon Grabski for technical assistance with the microscopy, Roxy Nickels for maintenance of the tobacco cultures, Marc Van Montagu for the SOD and catalase cDNA probes, and Jacqueline Fleck for the glutathione peroxidase cDNA probe. This work was supported by Department of Energy Grant DE FG02-ER-20021, National Science Foundation Grant IBM 9723573, and Department of Agriculture Grant 97-35304).

- Scandalios, J. G. (1993) *Plant Physiol.* **101**, 7–12.
- Beal, M. F. (1995) *Ann. Neurol.* **38**, 357–366.
- Boveris, A. & Cadenas, E. (1982) in *Superoxide Dismutase*, ed. Oberley, L. W. (CRC Press, Boca Raton, FL), pp. 15–30.
- Vanlerberghe, G. C. & McIntosh, L. (1997) *Annu. Rev. Plant Physiol. Plant Mol. Biol.* **48**, 703–734.
- Elthon, T. E. & McIntosh, L. (1987) *Proc. Natl. Acad. Sci. USA* **84**, 8399–8403.
- Umbach, A. L. & Siedow, J. N. (1993) *Plant Physiol.* **103**, 845–854.
- Vanlerberghe, G. C. & McIntosh, L. (1994) *Plant Physiol.* **105**, 867–874.
- Vanlerberghe, G. C. & McIntosh, L. (1992) *Plant Physiol.* **100**, 1846–1851.
- Vanlerberghe, G. C., Vanlerberghe, A. E. & McIntosh, L. (1994) *Plant Physiol.* **106**, 1503–1510.
- Vanlerberghe, G. C., Vanlerberghe, A. E. & McIntosh, L. (1997) *Plant Physiol.* **113**, 657–661.
- Purvis, A. C. (1997) *Physiol. Plant.* **100**, 165–170.
- Wagner, A. M. & Moore, A. L. (1997) *Biosci. Rep.* **17**, 319–333.
- Vanlerberghe, G. C. & McIntosh, L. (1992) *Plant Physiol.* **100**, 115–119.
- Lennon, A. M., Neuenschwander, U. H., Ribas-Carbo, M., Giles, L., Ryals, J. A. & Siedow, J. N. (1997) *Plant Physiol.* **115**, 783–791.
- Hiser, C. & McIntosh, L. (1990) *Plant Physiol.* **93**, 312–318.
- Prasad, T. K., Anderson, M. D., Marin, B. A. & Stewart, C. R. (1994) *Plant Cell* **6**, 65–74.
- Doke, N., Miura, Y., Sanchez, L. M. & Kawakita, K. (1994) in *Causes of Photooxidative Stress and Amelioration of Defense Systems in Plants*, eds. Foyer, C. H. & Mullineaux, P. M. (CRC Press, Boca Raton, FL), pp. 177–199.
- Olson, P. D. & Varner, J. E. (1993) *Plant J.* **4**, 887–892.
- Purvis, A. C. & Shewfelt, R. L. (1993) *Physiol. Plant.* **88**, 712–718.
- Zhu, H., Bannenberg, G. H., Moldeus, P. & Shertzter, H. G. (1994) *Arch. Toxicol.* **68**, 582–587.
- Grabski, S., de Feijter, A. W. & Schindler, M. (1993) *Plant Cell* **5**, 25–38.
- Köhlwer, R. H., Zipfel, W. R., Webb, W. W. & Hanson, M. R. (1997) *Plant J.* **11**, 613–621.
- Criqui, M. C., Jamet, E., Parmentier, Y., Marbach, J., Durr, A. & Fleck, J. (1992) *Plant Mol. Biol.* **18**, 623–627.
- Tsang, E., Bowler, C., Hérouart, D., Van Camp, W., Villarroel, R., Genetello, C., Van Montagu, M. & Inzé, D. (1991) *Plant Cell* **3**, 783–792.
- Örviar, B. L., McPherson, J. & Ellis, B. (1997) *Plant J.* **11**, 203–212.
- Ohshima, M., Matsuoka, M., Yamamoto, N., Tanaka, Y., Kano-Murakami, Y., Ozeki, Y., Kato, A., Harada, N. & Ohashi, Y. (1987) *FEBS Lett.* **10**, 243–246.
- Metz, A. M., Timmer, R. T. & Browning, K. S. (1992) *Gene* **120**, 313–314.
- Singh, N. K., Handa, A. K., Hasegawa, P. M. & Bressan, R. A. (1985) *Plant Physiol.* **79**, 126–137.
- Purvis, A. C., Shewfelt, R. L. & Gegogee, J. W. (1995) *Physiol. Plant.* **94**, 743–749.
- Pantopoulos, K., Mueller, S., Atzberger, A., Ansoerge, W., Stremmel, W. & Hentze, M. W. (1997) *J. Biol. Chem.* **272**, 9802–9808.
- Prasad, T. K., Anderson, M. D., Martin, B. A. & Stewart, C. R. (1994) *Plant Cell* **6**, 65–74.
- Minagawa, N., Koga, S., Nakano, M., Sakajo, S. & Yoshimoto, A. (1992) *FEBS Lett.* **302**, 217–219.
- Van Camp, W., Willekens, H., Bowler, C., Van Montagu, M. & Inzé, D., Reupold-Popp, P., Sandermann, H. & Langebartels, C. (1994) *Bio/Technology* **12**, 165–168.
- McKersie, B. D., Chen, Y., de Beus, M., Bowley, S. R., Bowler, C., Inzé, D., D'Halluin, K. & Botterman, J. (1993) *Plant Physiol.* **103**, 1155–1163.
- Bowler, C., Alliotte, T., De Loose, M., Van Montagu, M. & Inzé, D. (1989) *EMBO J.* **8**, 31–38.
- Kurepa, J., Hérouart, D., Van Montagu, M. & Inzé, D. (1997) *Plant Cell Physiol.* **38**, 463–470.
- Takahashi, H., Chen, Z., Du, H., Liu, Y. & Klessig, D. (1997) *Plant J.* **11**, 993–1005.
- Chen, Z., Silva, H. & Klessig, D. F. (1993) *Science* **262**, 1883–1886.
- Willekens, H., Langebartels, C., Tiré, C., Van Montagu, M., Inzé, D. & Van Camp, W. (1994) *Proc. Natl. Acad. Sci. USA* **91**, 10450–10454.
- McIntosh, L., Eichler, T., Gray, G., Maxwell, D., Nickels, R. & Wang, Y. (1998) *Biochim. Biophys. Acta* **1365**, 278–284.
- Popov, V. N., Simonian, R. A., Skulachev, V. P. & Starkov, A. A. (1997) *FEBS Lett.* **415**, 87–90.
- Hsiago, K.-C. & Bornman, C. H. (1993) *J. Exp. Bot.* **44**, 1847–1849.
- Quillet-Mary, A., Jaffrezou, J.-P., Mansat, V., Bordier, C., Naval, J. & Laurent, G. (1997) *J. Biol. Chem.* **272**, 21388–21395.
- Levine, A., Tenhaken, R., Dixon, R. & Lamb, C. (1994) *Cell* **79**, 583–593.
- Caro, A. & Puntarulo, S. (1996) *Biochim. Biophys. Acta* **1291**, 245–251.
- Wagner, A. M. (1995) *FEBS Lett.* **368**, 339–342.
- Chivasa, S. & Carr, J. P. (1998) *Plant Cell* **10**, 1489–1498.
- Kingston-Smith, A. H., Harbinson, J. & Foyer, C. H. (1999) *Plant Cell Environ.*, in press.